Journal of Experimental Botany, Vol. 61, No. 11, pp. 3137–3149, 2010
doi:10.1093/jxb/erq139 Advance Access publication 4 June, 2010
This paper is available online free of all access charges (see http://jxb.oxfordjournals.org/open_access.html for further details)

Journal of Experimental Botany
www.jxb.oxfordjournals.org

RESEARCH PAPER

A major grain protein content locus on barley (*Hordeum vulgare* L.) chromosome 6 influences flowering time and sequential leaf senescence

Joseph A. Lacerenza, David L. Parrott and Andreas M. Fischer*

Department of Plant Sciences and Plant Pathology, Montana State University, Bozeman, MT 59717-3150, USA

* To whom correspondence should be addressed. E-mail: fischer@montana.edu

Received 17 March 2010; Revised 28 April 2010; Accepted 29 April 2010

Abstract

Timing of various developmental stages including anthesis and whole-plant ('monocarpic') senescence influences yield and quality of annual crops. While a correlation between flowering/seed filling and whole-plant senescence has been observed in many annuals, it is unclear how the gene networks controlling these processes interact. Using near-isogenic germplasm, it has previously been demonstrated that a grain protein content (GPC) locus on barley chromosome 6 strongly influences the timing of post-anthesis flag leaf senescence, with high-GPC germplasm senescing early. Here, it is shown that the presence of high-GPC allele(s) at this locus also accelerates pre-anthesis plant development. While floral transition at the shoot apical meristem (SAM; determined by the presence of double ridges) occurred simultaneously, subsequent development was faster in the high- than in the low-GPC line, and anthesis occurred on average 5 d earlier. Similarly, sequential (pre-anthesis) leaf senescence was slightly accelerated, but only after differences in SAM development became visible. Leaf expression levels of four candidate genes (from a list of genes differentially regulated in post-anthesis flag leaves) were much higher in the high-GPC line even before faster development of the SAM became visible. One of these genes may be a functional homologue of *Arabidopsis* glycine-rich RNA-binding protein 7, which has previously been implicated in the promotion of flowering. Together, the data establish that the GPC locus influences pre- and post-anthesis barley development and senescence, and set the stage for a more detailed analysis of the interactions between the molecular networks controlling these important life history traits.

Key words: Barley (*Hordeum vulgare* L.), development, flowering time control, glycine-rich RNA-binding protein, leaf senescence, monocarpic senescence.

Introduction

Due to their influence on yield and quality parameters, plant developmental events such as inflorescence initiation, anthesis, and whole-plant senescence are of primary importance in annual crops (García del Moral *et al.*, 2002; Masclaux-Daubresse *et al.*, 2008). The last decade has seen substantial progress in our understanding of the molecular processes controlling these events; first in *Arabidopsis* (e.g. Buchanan-Wollaston, 1997; Noh and Amasino, 1999; Suárez-López *et al.*, 2001) and then, using this model species for comparison, in several annual crops including barley (e.g. Gregersen *et al.*, 2008; Jukanti *et al.*, 2008; Karsai *et al.*, 2008). It is well established that whole-plant ('monocarpic') senescence and death are linked with flowering and seed development in annual species (Lim *et al.*, 2007; Wingler *et al.*, 2010), but it is not clear how the gene networks controlling these processes interact. Several authors have observed that early-flowering plant lines were also early senescing, while no such connection was observed in other studies of monocarpic senescence, suggesting both flowering time-dependent and -independent inputs into

Abbreviations: GPC, grain protein content; GRP, glycine-rich RNA-binding protein; LRR, leucine-rich repeat; qRT-PCR, quantitative real-time reverse transcription-PCR; QTL, quantitative trait locus; SAM, shoot apical meristem.

senescence regulation (Hensel *et al.*, 1993; Kim *et al.*, 2004; Wu *et al.*, 2008; Wingler *et al.*, 2010).

Flower initiation and development in temperate grasses including barley are controlled by environmental cues, primarily by low temperatures (vernalization) and day length (Trevaskis *et al.*, 2007; Hemming *et al.*, 2008; Distelfeld *et al.*, 2009). Some of the important genes involved in perceiving and integrating these external signals include *vernalization1* (*vrn1*), *vrn2*, and *vrn3*/*HvFT1*, with *vrn3* apparently homologous to the *Arabidopsis flowering locus T* (*FT*) gene (Trevaskis *et al.*, 2007; Distelfeld *et al.*, 2009). Recent research indicates that the FT protein is synthesized in leaves under conditions conducive to flower initiation and transported to the shoot apex, where it is instrumental in the switch from vegetative to reproductive development (Corbesier *et al.*, 2007; Distelfeld *et al.*, 2009). Comparing *Arabidopsis* and barley, available data indicate that the molecular network involved in flower initiation is only partially conserved. Specifically, there is no barley homologue to the *Arabidopsis* flowering repressor gene *flowering locus C* (*FLC*), although *vrn2* may have partially analogous functions (Andersen *et al.*, 2004; Trevaskis *et al.*, 2007).

Research in the authors' laboratory is focused on barley leaf senescence and senescence-associated nitrogen remobilization. In this context, it has been demonstrated that a locus on barley chromosome 6, delineated by molecular markers ABG458 and HVM74, controls ~45% of the variation of grain protein content (GPC) and also influences the timing of post-anthesis senescence of the plant's topmost leaves, with high-GPC germplasm senescing faster (See *et al.*, 2002; Mickelson *et al.*, 2003; Heidlebaugh *et al.*, 2008; Jukanti and Fischer, 2008; Jukanti *et al.*, 2008). A homologous locus is present on wheat chromosome 6B; in that species, it has been demonstrated by map-based cloning that the high-GPC/fast-senescence phenotype is due to the presence of a functional NAC transcription factor, while the gene is deleted or truncated in low-GPC tetraploid or hexaploid germplasm (Uauy *et al.*, 2006). Extending the analysis to barley, Distelfeld *et al.* (2008) have demonstrated the presence of a homologous gene (*HvNAM-1*) at this locus, and identified sequence differences between barley varieties differing in GPC.

Transcriptomic comparison of near-isogenic (BC_4F_3) germplasm varying in the allelic state of this locus has identified several genes, which are highly (>10- to >100-fold) up-regulated in high- (fast senescence) as compared with low-GPC germplasm. These include two leucine-rich repeat (LRR) transmembrane protein kinases, a gene coding for a glycine-rich RNA-binding protein (GRP) with ~65% sequence identity with *Arabidopsis* GRP7 (AtGRP7; see Supplementary Fig. S1 available at *JXB* online) and slightly lower identity with AtGRP8, a gene coding for a putative lipase/thioesterase, and a gene of as yet unknown function (Jukanti *et al.*, 2008). Detailed bioinformatic analysis of one transmembrane protein kinase gene (for which a full-length cDNA is available) indicates its relationship with microbe/pathogen-associated molecular pattern receptors of the LRR–RLK XII type such as FLS2 (interacting with flagellin; Torii, 2008; Boller and Felix, 2009), thereby suggesting a role for this gene/protein in plant pathogen defence. Recent literature implicates AtGRP7 in output events from the circadian clock (Schöning *et al.*, 2007), in plant pathogen defence (Fu *et al.*, 2007), and in plant flowering control (Streitner *et al.*, 2008), suggesting a central regulatory role for this gene and its product. Of particular interest to the present study, Streitner *et al.* (2008) have recently demonstrated that *Arabidopsis* lines without AtGRP7 functionality [RNA interference (RNAi) and T-DNA insertion lines] flower somewhat later under long days and considerably later under short days when compared with corresponding wild-type germplasm. In addition, flowering was accelerated by overexpressing the gene. However, no influence of AtGRP7 function on plant development was found in vernalized plants.

While analysing post-anthesis senescence, it had repeatedly been observed that our low-GPC barley germplasm flowered on average 3–4 d later, and that pre-anthesis (sequential) leaf senescence progressed more slowly in low-GPC than in high-GPC lines grown under controlled conditions (mentioned in Jukanti and Fischer, 2008). While this effect was eliminated in post-anthesis senescence studies by basing comparative leaf analyses on days past anthesis (Jukanti *et al.*, 2008), the results obtained by Streitner *et al.* (2008) confirmed its importance. One of the main differences between low- and high-GPC germplasm is the difference in barley *GRP* expression (see above), suggesting functional homology of the *Arabidopsis* and barley *GRP* genes. This hypothesis is strengthened by the fact that differences in anthesis dates between low- and high-GPC lines were only visible in plant material grown under controlled conditions (with day/night temperatures never below ~15 °C), but not in field-grown material which experienced low to freezing temperatures during early plant development, resulting in mild vernalization [unpublished observations; additionally, no quantitative trait locus (QTL) for anthesis time point was found near the GPC QTL in the original mapping study by See *et al.* (2002)]. It therefore became imperative to (i) quantify differences in pre-anthesis development of low- and high-GPC barley germplasm, and (ii) to correlate developmental observations with expression levels of the genes discussed above, particularly with expression levels of the *GRP* gene. Data obtained from this study establish a solid foundation for the detailed analysis of molecular interactions between barley genes controlling floral transition and development (such as the *vrn* genes including *vrn3*/*HvFT1*) and whole-plant (monocarpic) senescence.

Materials and methods

Plant material, leaf development, anthesis dates, and non-destructive chlorophyll assays

Germplasm used in this study has been described in detail in Jukanti *et al.* (2008). Briefly, barley (*Hordeum vulgare* L.) variety

'Karl' is characterized by its low GPC under a variety of environmental conditions (See *et al.*, 2002; Mickelson *et al.*, 2003). Using four backcrosses (followed by marker-assisted selection) and selfing we derived several lines including '10_11' (BC4F3), which are near-isogenic to 'Karl', but contain high-GPC allele(s) from variety 'Lewis' at a locus on chromosome 6 (delineated by molecular markers ABG458 and HVM74), which controls both GPC and the timing of leaf senescence. Plants were grown from 'Karl' and '10_11' seeds in potting soil in 1 gallon pots (three plants per pot) in a growth room (Conviron, Winnipeg, Manitoba, Canada) with a 25/20 °C day/night temperature cycle under long-day conditions (16/8 h) and a light intensity of ~200 μE m^{-2} s^{-1}. Plants were fertilized with 250 ml of Peter's Professional General Purpose fertilizer (4 g l^{-1}; Scotts-Sierra Horticultural Products Company, Marysville, OH, USA) per 1 gallon pot with three plants at 2, 4, and 6 weeks after planting.

All leaves along the primary shoots of growing plants were tagged with the date on which full expansion occurred, from leaf 1 (the first, oldest leaf) to flag leaves (typically leaf 13). Full leaf expansion was defined as the day when auricles were developed. All tags were collected from mature (dead) plants at the end of the experiment, and leaf development was plotted in days after planting. Data were obtained from 26–68 'Karl' and '10_11' shoots for leaves 1–13; 12 'Karl' and five '10_11' shoots for leaf 14 (reflecting the fact that most shoots, especially in '10_11', only produce 13 leaves), and three shoots for leaf 15 (in 'Karl' only).

Anthesis dates were defined as the day when awns first appeared above the flag leaf blade, for both primary shoots and tillers of each plant. Data were calculated from 30 primary shoots and 160 tillers.

Non-destructive chlorophyll analyses were performed with a Minolta SPAD-502 (Konica Minolta Sensing, Osaka, Japan) chlorophyll meter. For each assayed leaf, three separate measurements were taken from an area ~3 cm in length in the middle of the leaf blade, averaged, and noted. Means, standard deviations, and Student's *t*-tests (see below) were calculated from 20–50 leaves for each data point.

Analysis of shoot apical meristem (SAM) development

To follow SAM development, primary shoots were harvested between 8 d and 49 d after planting, dissected under a low-magnification stereoscopic microscope (model DC5-420TH, National Optical and Scientific Instruments Inc., San Antonio, TX, USA), and meristems were documented with the attached digital camera.

Chlorophyll assays (destructive), amino acids, nitrate, and total nitrogen

For all assays described in this and the following paragraphs, leaf samples (consisting of three leaves each) were shock-frozen in liquid nitrogen and stored at –80 °C until analysis. They were then ground to a fine powder using a pestle and mortar, again in liquid nitrogen. Chlorophylls were extracted from liquid nitrogen powder with 80% acetone. Extracts were centrifuged (5 min, 21 000 *g*, 4 °C), and supernatants were assayed spectrophotometrically at 649 nm and 665 nm. Chlorophyll contents were calculated using the formulas published by Strain *et al.* (1971). Amino acids (soluble α-amino nitrogen) and nitrates were determined from hot water extracts, as described by Mickelson *et al.* (2003). Total nitrogen was quantified through a combustion method with a LECO FP-528 nitrogen analyser (LECO Corp., St Joseph, MO, USA). Means, standard deviations, and Student's *t*-tests (see below) were calculated from three or four independently extracted samples, each consisting of three leaves for all these analyses.

SDS–PAGE and immunoblotting

Soluble and membrane proteins were extracted from leaves (liquid nitrogen powder) and analysed by SDS–PAGE and immunoblotting as described by Parrott *et al.* (2007). Samples loaded in each gel lane corresponded to 3.5 mg fresh weight and were derived from nine (3×3) leaves to alleviate leaf to leaf variation. For immunoblotting, proteins were electrotransferred to nitrocellulose, and membranes were blocked and probed with 1:10 000 diluted antibodies specific for the N-terminus of the large subunit of Rubisco (see Parrott *et al.*, 2007 for a description of these antibodies). Secondary antibodies were a goat anti-rabbit IgG–horseradish peroxidase conjugate (Bio-Rad, Hercules, CA, USA) diluted 1: 10 000 before use. Blots were incubated with chemiluminescent substrate (SuperSignal West Pico Chemiluminescent Substrate, Pierce, Rockford, IL, USA) for 10 min before exposure to X-ray film.

Gene expression analysis

Transcript levels of five genes, which were strongly up-regulated in flag leaves of '10_11' as compared with 'Karl' at 14 d and 21 d past anthesis (Jukanti *et al.*, 2008), were measured by quantitative real-time RT-PCR (qRT-PCR) in selected leaves at 21, 35, 42, and 56 d after planting. Additionally, expression levels of *HvNAM-1* (DQ869678) were also determined in some of these leaves, for reasons outlined in the Introduction. Specific primers used for each analysed gene as well as low and high standards are shown in Supplementary Table S1 at *JXB* online. Contig numbers refer to the Affymetrix Barley Genome Array [Close *et al.* (2004); accessible through the HarvEST Barley database (http://harvest.ucr.edu/; Close *et al.*, 2007]. For primers which were used for the first time in this study (*HvNAM-1* and a new primer set for *GRP*), specificity and product length were verified by agarose gel electrophoresis.

RNA extractions were performed as described in Parrott *et al.* (2007), and RNA quality was tested using an RNA 6000 Nano assay (Bioanalyzer 2100, Agilent Technologies, Palo Alto, CA, USA). A RotorGene 3000 thermal cycler (Corbett Life Science, Mortlake, NSW, Australia) was used for PCR with the following cycling profile: 50 °C for 2 min, 95 °C for 2 min, 40 cycles of 94 °C for 5 s, 55 °C for 15 s, and 72 °C for 15 s, and a melt curve from 72 °C to 95 °C following PCR cycling. All PCR data were analysed using Rotor Gene 6 (Corbett Life Science) software. Means and standard deviations are shown for three independently extracted samples (each derived from three leaves) for each data point.

Statistical analysis

Student's *t*-tests (two-sided) were performed using the corresponding function in Microsoft Excel 2007 for Windows (Microsoft Corporation, Redmond, WA, USA) for most parameters to determine if differences between 'Karl' and '10_11' were significant. No statistics were calculated for gene expression analyses, as expression levels differed by several orders of magnitude between 'Karl' and '10_11' for all data points in Figs 8–11.

Results

Differences in anthesis dates were previously observed when comparing the low-GPC barley variety 'Karl' with a near-isogenic line ('10_11') containing the high GPC locus, with 'Karl' flowering somewhat later. Similarly, anthesis occurred earlier in the high-GPC variety 'Lewis' as compared with a low-GPC near-isogenic line, '21_7' (Jukanti and Fischer, 2008). To explore these differences systematically, 'Karl' and '10_11' were grown under controlled conditions, as described under Materials and methods.

Full leaf emergence was determined by the development of auricles on primary shoot leaves. No systematic

differences between 'Karl' and '10_11' were observed until the full development of the seventh leaf (with leaf 1 the oldest, first developed leaf) at ~36 d after planting (Fig. 1A). However, starting with leaf 8, and throughout the rest of plant development, leaf development in 'Karl' was significantly delayed [on average by 2.1 d for leaf 8; 2.8 d for leaf 9; 2.6 d for leaf 10; 2.8 d for leaf 11; 4.6 d for leaf 12; 3.1 d for leaf 13 (the only non-significant difference); and 7.2 d for leaf 14] (Fig. 1A). A majority of 'Karl' and '10_11' shoots had 13 leaves (i.e. leaf 13 was the flag leaf), but emergence of a 14th leaf was about twice as frequent in 'Karl' as in '10_11', and only (very few) 'Karl' shoots developed 15 leaves on their main shoots, underlining again their slower development.

Consistently with leaf development, anthesis (determined by the emergence of awns above the flag leaf blade) was delayed in 'Karl', with both main shoots and tillers flowering on average 5 d later than in '10_11' (differences are highly significant; Fig. 1B).

Later anthesis dates suggested that inflorescence initiation at the SAM might also occur later in 'Karl' than in '10_11'. However, microscopic observation demonstrated that this transition occurred between 15 d and 21 d after planting for both lines (Fig. 2). The development of double ridges (DRs) is considered a reliable indicator of inflorescence initiation (García del Moral *et al.*, 2002), and such structures can be clearly observed in both 'Karl' and '10_11' by 21 d after planting (Fig. 2E, F). Further development towards the 'triple mound' stage, allowing distinction of central and lateral spikelet primordia (cs and ls) after 28 d, still occurred largely in parallel (Fig. 2G, H). However, between 28 d and 35 d, a clear difference in SAM development was observed: while 'Karl' was still at the 'triple mound' stage at 35 d, '10_11' had proceeded further towards the 'stamen primordium' stage (compare with García del Moral *et al.*, 2002; Babb and Muehlbauer, 2003). In addition, there was also a clear size difference (compare scale bars in Fig. 3A and B). Differences were also visible at 42 d (Fig. 3C, D) and 49 d (Fig. 3E, F), with '10_11' again faster at reaching the 'awn primordium' (aw) stage. Clearly, therefore, while inflorescence initiation occurred simultaneously in 'Karl' and '10_11', the allelic state of the GPC locus influenced later stages of inflorescence development.

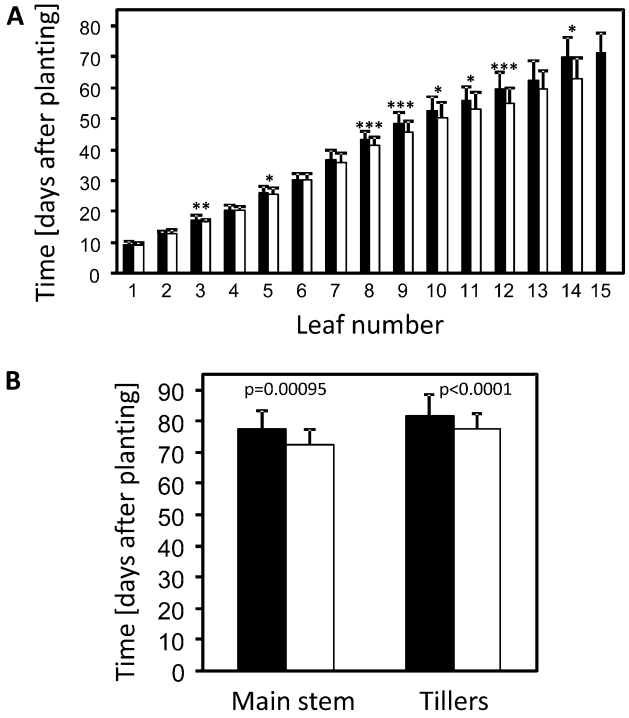

Fig. 1. Plant development. (A) The time points of full leaf emergence were compared in 'Karl' (black columns) and '10_11' (white columns). Leaf 1 is the first, oldest leaf, with subsequent numbers designating the leaf sequence along the primary shoot. (B) Anthesis dates were compared in main shoots and tillers of 'Karl' (black columns) and '10_11' (white columns). Means and standard deviations of 26–68 main shoots are shown for leaves 1–13 in A. Means and standard deviations of 30 main shoots and 160 tillers are shown in B. Student's *t*-tests were performed to determine significant differences between 'Karl' and '10_11' for both A and B. **P* <0.05; ***P* <0.01; ****P* <0.001.

As pre-anthesis differences in (sequential) leaf senescence had previously been observed, non-destructive leaf chlorophyll assays were next performed using a Minolta chlorophyll meter (as described under Materials and methods). These assays, while suggesting minor differences between 'Karl' and '10_11' leaves prior to the onset of chlorophyll loss/leaf senescence, did not indicate faster senescence of the first three leaves in '10_11', which were completely senesced by 42 d after planting (Fig. 4A–C). However, careful inspection of leaves 4 and 5 at 42 d indicates small, significant differences between 'Karl' and '10_11' during the phase of rapid chlorophyll loss (Fig. 4D, E), and analysis of leaves 7–12 between 56 d and 84 d clearly confirmed faster senescence of '10_11' leaves (with anthesis occurring at ~73 d in '10_11' and 78 d in 'Karl' primary shoots). Due to the fact that not all shoots developed the same number of leaves (possibly leading to comparisons of leaves which are not identical relative to the position of the developing ear), some analyses were also performed after flag leaf emergence (Supplementary Fig. S2 at *JXB* online), measuring chlorophyll levels of flag leaves (leaves immediately below the ear), and second and third leaves below the ear. These assays again confirmed faster leaf senescence in '10_11' and corroborated data from a previous analysis of post-anthesis leaf senescence (Heidlebaugh *et al.*, 2008; Jukanti *et al.*, 2008).

Based on data from the Minolta chlorophyll meter assays, more detailed biochemical (destructive) analyses were performed for several time points. First, chlorophyll levels (Fig. 5) were determined in leaves 1–4 at 21 d and in leaves 1–5 at 35 d after planting, and in selected leaves at 42 d and 56 d (when older leaves were already fully senesced in both lines). These assays did not demonstrate any significant differences in leaf chlorophyll levels during the first 5 weeks of plant development, thus confirming data shown in Fig. 4. However, at both 42 d and 56 d after planting, chlorophyll levels of older '10_11' leaves were

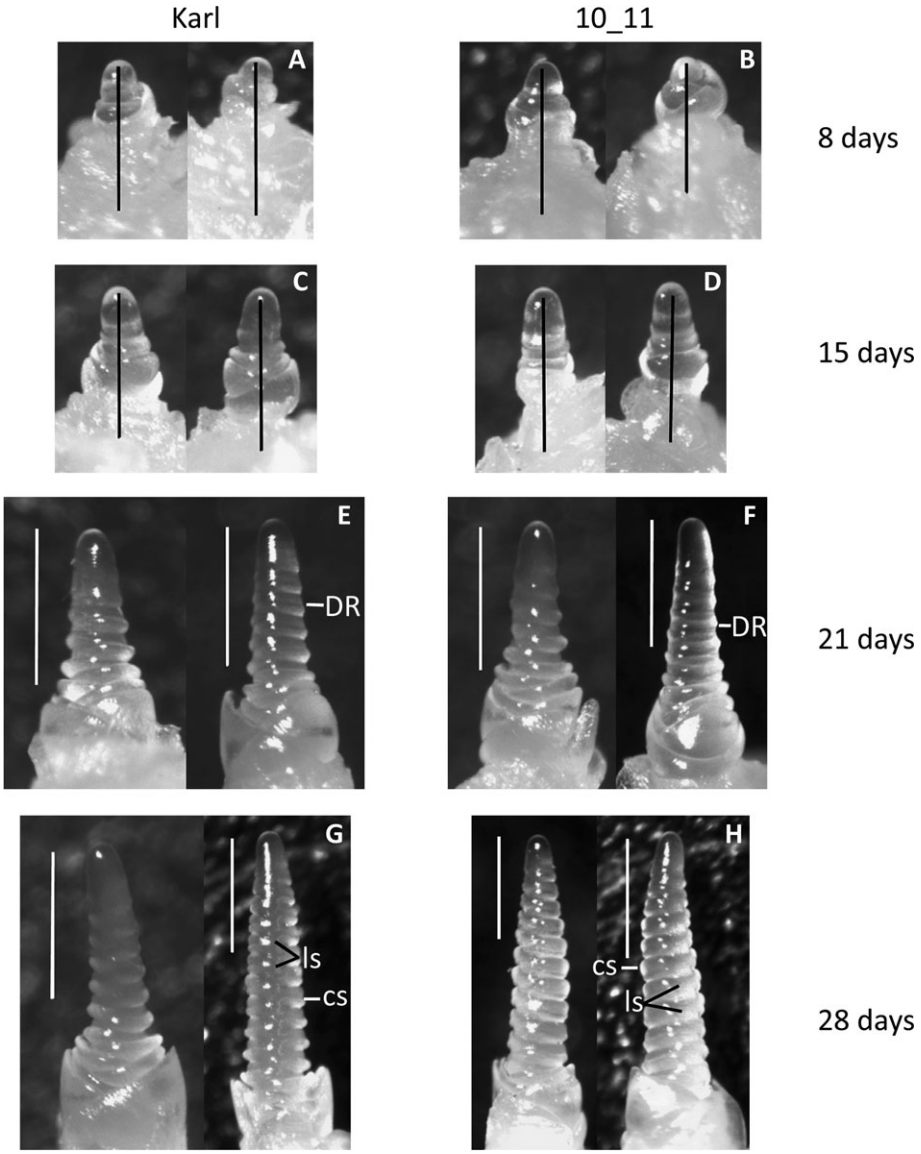

Fig. 2. Development of shoot apical meristems (SAMs) from 8 d to 28 d after planting. SAMs were compared in 'Karl' and '10_11' by stereomicroscopic observation at 8 d (A, B), 15 d (C, D), 21 d (E, F), and 28 d (G, H). The length of the bar is 500 μm. DR, double ridge; cs, central spikelet; ls, lateral spikelet.

lower than the corresponding leaves in 'Karl', confirming that accelerated senescence becomes detectable ~6 weeks after planting. SDS–PAGE analyses for both soluble and membrane proteins, and Rubisco immunoblot analyses were performed to characterize further the differences in pre-anthesis senescence (Fig. 6). As for chlorophylls, no differences in leaf protein levels were observed between 'Karl' and '10_11' at 21 d. Protein levels were also similar at 35 d; while leaf 2 in '10_11' contained more soluble protein, the trend was opposite for membrane proteins. However, starting at 42 d, SDS–polyacrylamide gels and immunoblots indicated lower soluble protein, Rubisco, and membrane protein levels in older leaves of line '10_11' (leaf 5 at 42 d and leaf 7 at 56 d), confirming faster leaf senescence in this high-GPC line. Similar protein and chlorophyll levels were observed in younger 'Karl' and '10_11' leaves (before senescence initiation), such as leaves 6 and 7 at 42 d, and leaves 8 and 9 at 56 d (Figs 5C, D, 6D, F, I, J). The presented data also show how sequential leaf senescence progresses over time; while leaf 7 has just developed at 42 d (Figs 1, 4), it has started to senesce by 56 d (compare data for this leaf in Figs 4–6).

Previous analyses of post-anthesis senescence and N metabolism indicated differences in nitrogen compounds between low- and high-GPC lines (Heidlebaugh *et al.*, 2008). Therefore, nitrate, amino acid, and total nitrogen levels were compared in the leaves analysed for senescence parameters (above). For nitrates, these data indicated a trend towards higher levels in some 'Karl' leaves at 35 d and 42 d, just prior to and at the time point when senescence differences first become detectable (Fig. 7). In contrast, and also in contrast to post-anthesis analyses, amino acid (Supplementary Fig. S3) and total N levels (Supplementary Fig. S4) were not significantly different,

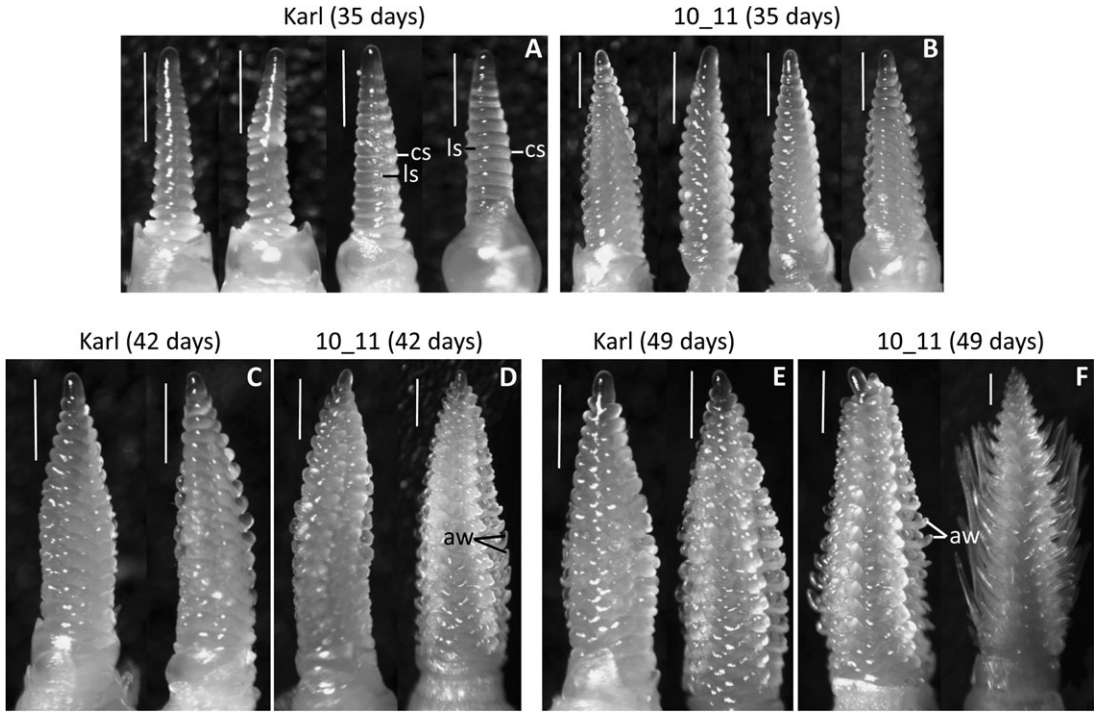

Fig. 3. Development of shoot apical meristems (SAMs) from 35 d to 49 d after planting. SAMs were compared in 'Karl' and '10_11' by stereomicroscopic observation at 35 d (A, B), 42 d (C, D), and 49 d (E, F). The length of the bar is 500 μm. cs, central spikelet; ls, lateral spikelet; aw, awn primordium.

with the exception of one (total nitrogen) or two (amino acids) data points at 21 d after planting (well before differences in senescence behaviour became measurable).

Based on data presented in Jukanti *et al.* (2008), it was hypothesized that the genes briefly described in the Introduction (coding for two LRR transmembrane protein kinases, a GRP, a putative lipase/thioesterase, and a gene with unknown function) are part of the signalling network controlling faster senescence in high-GPC germplasm (such as line '10_11'). It was further hypothesized that these differences might become measurable just before or around the time when differences in senescence behaviour between 'Karl' and '10_11' are first detected. For contigs rbaal9i05_at and 6206_s_at, coding for LRR transmembrane protein kinases, transcript levels differed by several orders of magnitude in all leaves investigated at 21, 35, 42, and 56 d after planting (please note the use of different *y*-axis scales for 'Karl' and '10_11' data in Figs 8 and 9). These differences were therefore measurable well before differences in SAM development or leaf senescence occurred. Furthermore, while contig 6206_s_at transcript levels were overall higher than those of rbaal9i05_at, expression patterns were largely parallel in '10_11', as previously observed in post-anthesis leaves (Jukanti *et al.*, 2008). As a molecular interaction between transmembrane protein kinases in plant signalling has previously been demonstrated (Boller and Felix, 2009), our cumulative data showing co-expression of these two genes in high-GPC germplasm suggest that they might be functionally important in the same signalling pathway, possibly by direct interaction at a membrane surface.

An *Arabidopsis* homologue of contig17116_at, AtGRP7, has previously been implicated in flowering time control through the autonomous pathway (Streitner *et al.*, 2008; see Introduction). Similarly to the two LRR transmembrane protein kinase genes, our data demonstrated a difference of around three orders of magnitude in the expression of this gene between 'Karl' and '10_11' in all analysed leaves (Fig. 10). In addition, especially in line '10_11', expression was typically higher in older leaves (such as leaf 1 at 21 d and leaf 4 at 35 d). The high expression levels in leaf 4 of '10_11' at 35 d, just before differences in senescence become measurable (and when SAMs are already different), is conspicuous, and correlates expression of this gene to the faster development occurring in line '10_11' at ~35 d.

Extensive database searches have so far not identified homologous proteins, or conserved protein domains, for the gene/contig shown in Fig. 11 (HA11K18u_s_at). Interest in this gene stems from the fact that a previous, post-anthesis transcriptomic analysis of 'Karl' and '10_11' has demonstrated that it not only is highly up-regulated in '10_11' as compared with 'Karl' leaves, but also is the most highly up-regulated gene in developing '10_11' kernels, i.e. it is up-regulated in both sources and sinks. Data presented here show that it is also strongly up-regulated in pre-anthesis '10_11' leaves. The most conspicuous analysis date for this gene is 35 d after planting (Fig. 11B), as it reaches its highest expression levels in older leaves at the same time, when differences in the rates of SAM development become obvious, and ~7 d before measurable differences in leaf senescence (see Figs 3–6). Similarly to the *GRP* gene (Fig. 10),

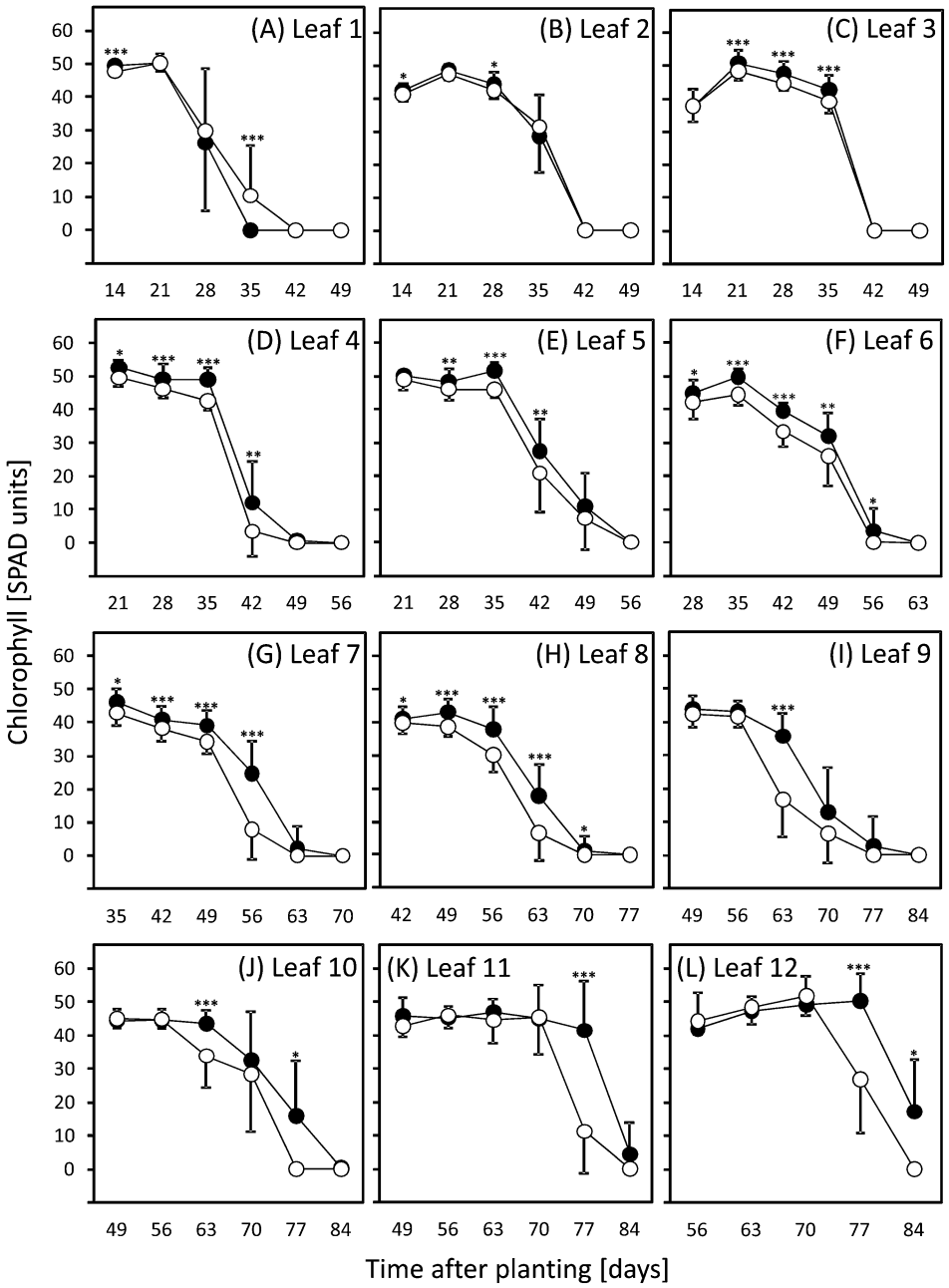

Fig. 4. Chlorophyll levels measured with a Minolta SPAD chlorophyll meter. Chlorophylls were compared in leaves 1 (A; first, oldest leaf) to 12 (L) of 'Karl' (filled circles) and '10_11' (open circles) as outlined in the Materials and methods. Means and standard deviations of 20–50 leaves are shown for each data point from 14 d to 70 d after planting, while *n* was lower (6–10) for 77 d and 84 d. Student's *t*-tests were performed to determine significant differences between 'Karl' and '10_11'. **P* <0.05; ***P* <0.01; ****P* <0.001.

this gene may therefore be part of the signalling network controlling faster development of '10_11' after this time point.

In contrast to the genes quantified in Figs 8–11, important differences in contig 7285_at (coding for a lipase/thioesterase) expression between 'Karl' and '10_11' were limited to post-anthesis leaves (Fig. 12; Jukanti *et al.*, 2008). Moreover, expression of this gene was lower in 35 d material than at the other time points; this finding does not support an important function for this gene in the faster development of '10_11'. Data presented in Fig. 12, with similar gene expression levels in 'Karl' and '10_11', also confirm that the highly differential expression shown for the other genes (in Figs 8–11) is not due to differences in the quality of extracted RNA.

As data obtained by Distelfeld *et al.* (2008) suggest that differences in *HvNAM-1* (DQ869678) sequence or regulation constitute the molecular basis for allelic differences at the barley GPC locus (see the Introduction), expression of this gene was also surveyed by qRT-PCR. Data obtained for several leaves at 21, 35, 42, and 56 d after planting showed very low (from undetectable to 0.0058 in the scale used for Figs 8–12), and essentially identical expression levels in both 'Karl' and 10_11' (not shown). These data

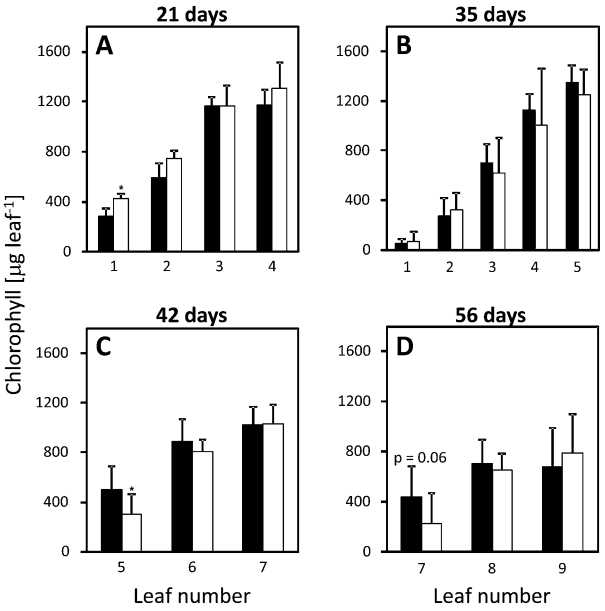

Fig. 5. Biochemical chlorophyll assays. Chlorophylls were extracted with acetone and quantified spectrophotometrically from selected leaves of 'Karl' (black columns) and '10_11' (white columns) at 21 (A), 35 (B), 42 (C), and 56 d (D) after planting, with leaf 1 representing the first, oldest main shoot leaf. Means and standard deviations of three or four replications are shown for each data point. Student's *t*-tests were performed to determine significant differences between 'Karl' and '10_11'. $^*P < 0.05$.

indicate that *HvNAM-1* transcript levels are not important for the developmental differences described here (but do not exclude control mechanisms related to HvNAM-1 protein function, quantity, and stability).

Discussion

The barley locus under investigation in this research was first identified as a QTL important for GPC (See *et al.*, 2002; Mickelson *et al.*, 2003). Subsequent work in our laboratory demonstrated a functional correlation between GPC and the timing of post-anthesis leaf senescence (Heidlebaugh *et al.*, 2008; Jukanti and Fischer, 2008; Jukanti *et al.*, 2008), and transcriptomic analyses have identified several genes which are highly up-regulated in senescing '10_11' as compared with 'Karl' leaves (Jukanti *et al.*, 2008). These genes may therefore participate in the signalling network regulating the senescence process.

Research presented here clearly demonstrates an influence of the GPC locus on pre-anthesis plant development. While the low-GPC variety 'Karl' was compared with only one high-GPC near-isogenic line (BC_4F_3; '10_11'), earlier anthesis was previously observed in the high-GPC variety 'Lewis' as compared with a low-GPC near-isogenic line ('21_7') (Jukanti and Fischer, 2008), thereby corroborating the detailed data presented here. The most important piece of information gained from the present results is the fact that 'Karl' and '10_11' development occur at the same rate until ~28 d after planting (in the culture system used here). The first difference is visible at the SAM: while floral transition and further development to the 'triple mound' stage occurred simultaneously in 'Karl' and '10_11' (Fig. 2), '10_11' developed faster after that time point. Specifically, at 35 d, '10_11' SAMs had progressed to the 'stamen primordium' stage, and they were also faster than 'Karl' at reaching the 'awn primordium' stage at 42 d (Fig. 3). By 42 d after planting, differences in leaf senescence became measurable, starting with leaves 4 and 5 (Figs 4–6). Therefore, a particular stage during early plant/inflorescence development needs to be reached before the GPC locus is able to influence further plant development and sequential leaf senescence. On a molecular level, this could depend on the activation (or inactivation) of a single gene, or on a more complex gene network. The *GRP* gene (Fig. 10) and especially the gene of unknown function (Fig. 11) quantified in this study may be important in this context, as they are both most highly expressed in older leaves at 35 d.

Our data also indicate differences in N metabolism between post-anthesis flag leaf senescence and pre-anthesis sequential leaf senescence. While leaf total N and amino acid levels were lower and/or decreased faster in '10_11' than in 'Karl' flag leaves (Heidlebaugh *et al.*, 2008), the present analysis detected no significant differences in these parameters in leaf 5 at 42 d or in leaf 7 at 56 d (Supplementary Figs S3, S4 at *JXB* online). Additionally, while nitrate levels were higher in '10_11' than in 'Karl' flag leaves at 7–28 d past anthesis, at least under high N fertilization (Heidlebaugh *et al.*, 2008), data presented in Fig. 7 indicated no significant differences in leaf 5 at 42 d and in leaf 7 at 56 d, but higher nitrate levels in younger (non-senescing) 'Karl' than '10_11' leaves at 35 d and 42 d. Therefore, while leaf senescence in '10_11' occurs faster both pre- and post-anthesis, there are clear differences in leaf N metabolism between the two developmental stages. A reasonable explanation for these differences is the presence of a strong reproductive sink in post-anthesis plants.

The fact that ~1000-fold differences are measurable between 'Karl' (low) and '10_11' (high) in the expression levels of the *GRP* gene is intriguing (Fig. 10, and Jukanti *et al.*, 2008 for post-anthesis data). The product of this gene is highly similar to AtGRP7, even more so in the RNA-binding than in the glycine-rich domain (Supplementary Fig. S1 at *JXB* online). Based on this sequence comparison and on the fact that in both barley (Figs 1–3) and *Arabidopsis* (Streitner *et al.*, 2008), plants with reduced *GRP* functionality developed more slowly, it is reasonable to postulate functional homology for the genes from the two species. Furthermore, Streitner *et al.* (2008) have demonstrated that vernalization negates the influence of AtGRP7 on plant development; the same may be true in barley, as the lines used in the present study demonstrated identical anthesis dates when grown in the field (as mentioned in the Introduction). Using vernalization and additional data, Streitner *et al.* (2008) demonstrated that AtGRP7 influences *Arabidopsis* development through the autonomous pathway, modifying expression levels of *FLC*.

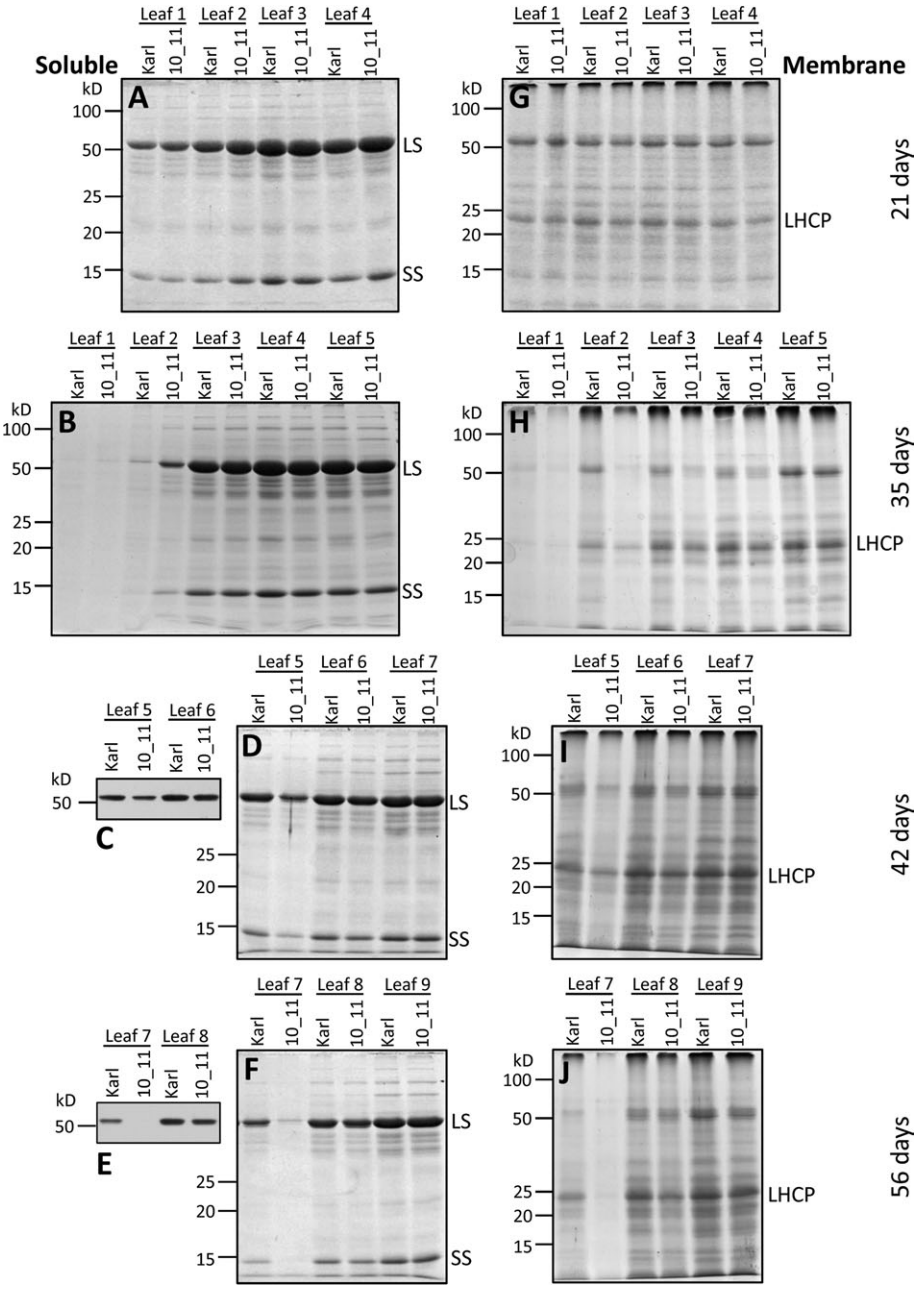

Fig. 6. Analysis of leaf protein levels. Soluble (A, B, D, F) and membrane proteins (G, H, I, J) were compared in selected leaves of 'Karl' and '10_11' by SDS–PAGE analysis at 21 (A, G), 35 (B, H), 42 (D, I), and 56 d (F, J) after planting, with leaf 1 representing the first, oldest main shoot leaf. At 42 d and 56 d, levels of the large subunit of Rubisco were compared by immunoblotting (C, E). Each lane in A–J was loaded with a sample corresponding to 3.5 mg fresh weight. LS, SS, large and small subunits of Rubisco; LHCP, light-harvesting chlorophyll-binding protein.

While barley has no gene which is homologous to *FLC*, other parts of the signalling network controlling plant transition to reproductive development are conserved between *Arabidopsis* and temperate grasses. We therefore hypothesized that the barley GRP interacts with the pathways controlled by *vrn1/2*, ultimately modifying *vrn3/HvFT1* gene expression and development of the SAM. In this context, it is noteworthy that Hemming *et al.* (2008) have demonstrated an influence of *HvFT* on inflorescence initiation and subsequent stages of inflorescence development, i.e. after the transition from a vegetative to a reproductive meristem has occurred. Our previous data also point to a possible role for *FT* genes in later plant developmental stages, as Jukanti *et al.* (2008) (see supplementary data to that manuscript) have demonstrated a 2- to 12-fold up-regulation of *FT* and *MFT* (*'mother of FT'*) genes in '10_11' leaves at 2 and 3 weeks past anthesis.

The most interesting aspect of the work presented here is the connection between the regulation of early plant development and the regulation of both sequential and whole-plant/monocarpic senescence. No such connection has been described by Streitner *et al.* (2008) in *Arabidopsis*

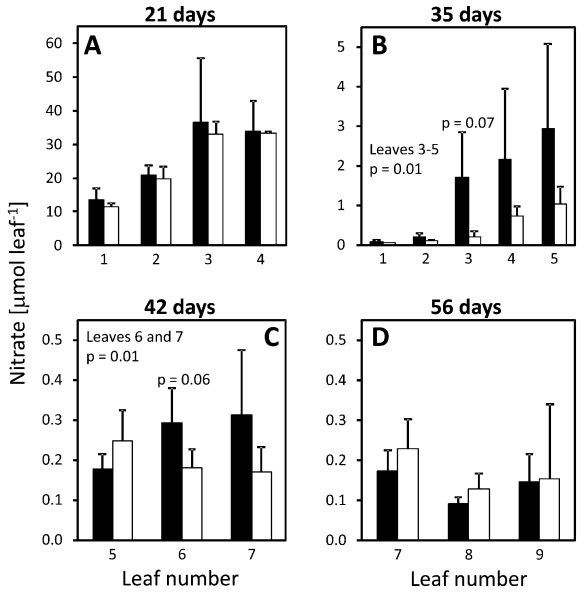

Fig. 7. Nitrate analysis. Nitrate was extracted and quantified in leaves of 'Karl' (black columns) and '10_11' (white columns) at 21 (A), 35 (B), 42 (C), and 56 d (D) after planting, with leaf 1 representing the first, oldest main shoot leaf. Means and standard deviations of three or four replications are shown for each data point. Student's *t*-tests were performed to determine significant differences between 'Karl' and '10_11'.

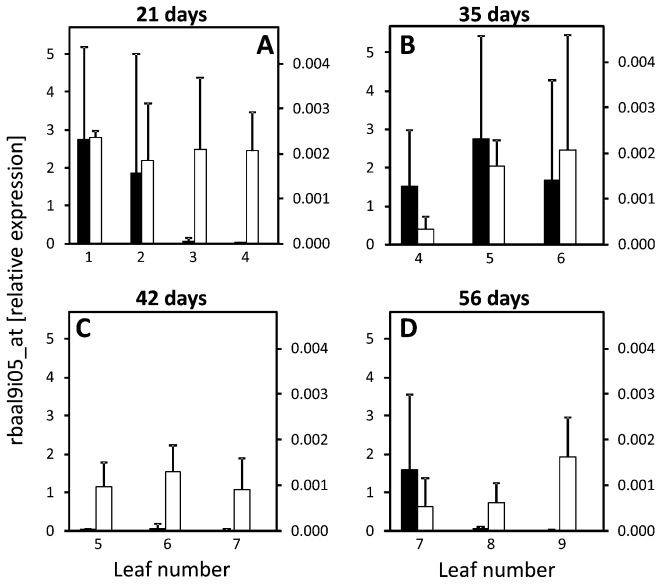

Fig. 8. Gene expression analysis of contig rbaal9i05_at, coding for a leucine-rich repeat transmembrane protein kinase. Expression levels were determined in selected leaves of 'Karl' (black columns) and '10_11' (white columns) at 21 (A), 35 (B), 42 (C), and 56 d (D) after planting by qRT-PCR using gene-specific primers, with leaf 1 representing the first, oldest main shoot leaf. Note that different scales were used to plot gene expression in 'Karl' (scale on the right of each graph) and '10_11' (scale on the left of each graph). Means and standard deviations of three biological replications are shown.

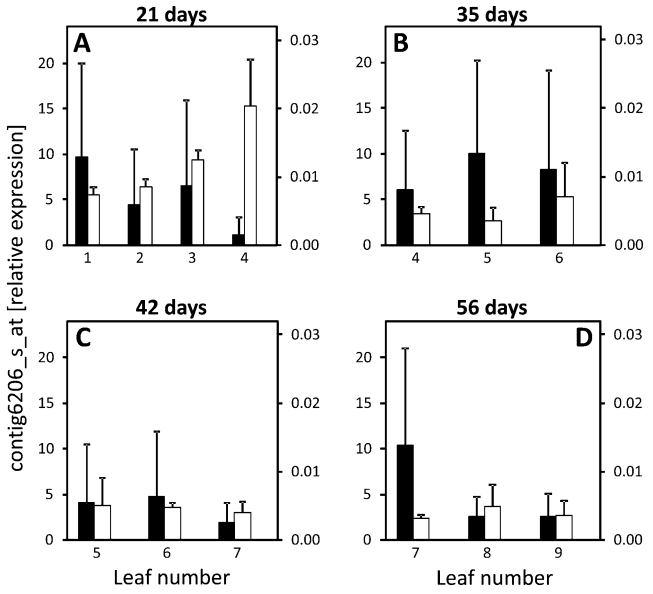

Fig. 9. Gene expression analysis of contig 6206_s_at, coding for a leucine-rich repeat transmembrane protein kinase. Expression levels were determined in selected leaves of 'Karl' (black columns) and '10_11' (white columns) at 21 (A), 35 (B), 42 (C), and 56 d (D) after planting by qRT-PCR using gene-specific primers, with leaf 1 representing the first, oldest main shoot leaf. Note that different scales were used to plot gene expression in 'Karl' (scale on the right of each graph) and '10_11' (scale on the left of each graph). Means and standard deviations of three biological replications are shown.

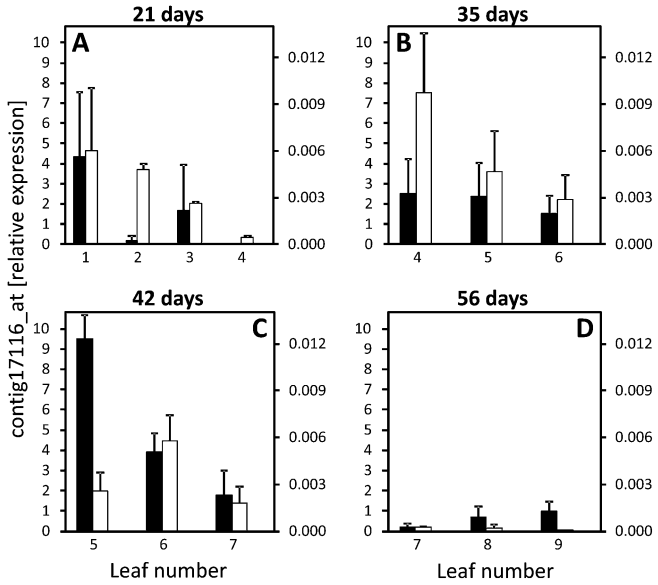

Fig. 10. Gene expression analysis of contig 17116_at, coding for a glycine-rich RNA-binding protein. Expression levels were determined in selected leaves of 'Karl' (black columns) and '10_11' (white columns) at 21 (A), 35 (B), 42 (C), and 56 d (D) after planting by qRT-PCR using gene-specific primers, with leaf 1 representing the first, oldest main shoot leaf. Note that different scales were used to plot gene expression in 'Karl' (scale on the right of each graph) and '10_11' (scale on the left of each graph). Means and standard deviations of three biological replications are shown.

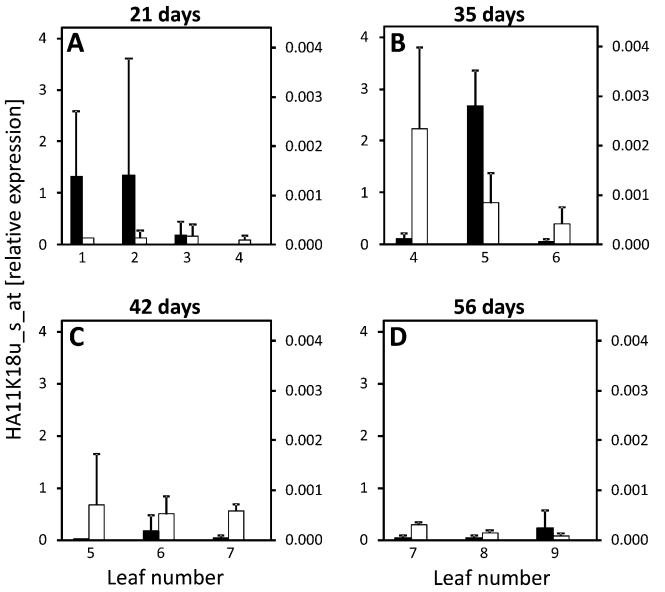

Fig. 11. Gene expression analysis of contig HA11K18u_s_at (unknown function). Expression levels were determined in selected leaves of 'Karl' (black columns) and '10_11' (white columns) at 21 (A), 35 (B), 42 (C), and 56 d (D) after planting by qRT-PCR using gene-specific primers, with leaf 1 representing the first, oldest main shoot leaf. Note that different scales were used to plot gene expression in 'Karl' (scale on the right of each graph) and '10_11' (scale on the left of each graph). Means and standard deviations of three biological replications are shown.

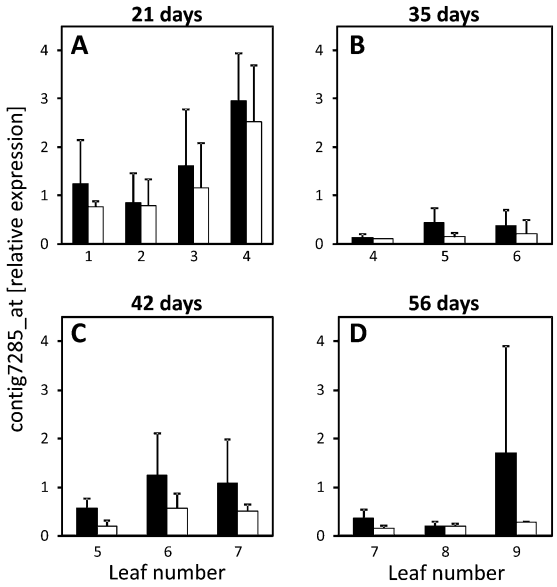

Fig. 12. Gene expression analysis of contig 7285_at, coding for a putative lipase/thioesterase. Expression levels were determined in selected leaves of 'Karl' (black columns) and '10_11' (white columns) at 21 (A), 35 (B), 42 (C), and 56 d (D) after planting by qRT-PCR using gene-specific primers, with leaf 1 representing the first, oldest main shoot leaf. In contrast to Figs 8–11, the same scale is used to plot expression levels of this gene for both 'Karl' and '10_11'. Means and standard deviations of three biological replications are shown.

lines differing in AtGRP7 levels, but Wingler *et al.* (2010), also working with *Arabidopsis*, have demonstrated that the *FRI* and *FLC* genes are important for the timing of whole-plant senescence in non-vernalized plants. While gene hierarchies remain unclear (do the same gene networks directly control both inflorescence development and sequential leaf senescence starting at ~35 d after planting, or are the latter dependent on the former?), experiments including vernalization and short-day treatments followed by the analysis of *vrn* and other genes (such as *ppd1* and *CO*) may allow important insights. The fact that post-anthesis differences in leaf senescence were maintained in field-grown material while differences in anthesis date were not (unpublished observations; see the Introduction) indicates that this line of experiments is promising.

In summary, data in this manuscript demonstrate that the GPC locus on barley chromosome 6 influences plant development and leaf senescence well before anthesis, but only after floral transition at the SAM has occurred. Additionally, data presented here in connection with recent literature results point to an experimental strategy which may allow us to unravel the molecular networks controlling early plant, including inflorescence, development, leaf senescence, and their interaction.

Supplementary data

Supplementary data are available at *JXB* online.

Figure S1. Sequence alignment of AtGRP7 (NM_179686) and contig 17116_at.

Figure S2. Chlorophyll levels of flag leaves, second, and third leaves measured with a Minolta SPAD chlorophyll meter.

Figure S3. Amino acid analysis.

Figure S4. Total nitrogen analysis.

Table S1. Gene-specific primer sequences used for expression analysis.

Acknowledgements

The authors would like to thank Dr U. Feller (Institute of Plant Sciences, University of Bern, Switzerland) for supplying the Rubisco antibodies used in Fig. 6. This work was supported by grants from the US Department of Agriculture-National Research Initiative (grant number 2005-02022), from the US Barley Genome Project, and from the Montana Board of Research & Commercialization Technology to AMF. Additional support from the Montana Agricultural Experiment Station is also gratefully acknowledged.

References

Andersen CH, Jensen CS, Petersen K. 2004. Similar genetic switch systems might integrate the floral inductive pathways in dicots and monocots. *Trends in Plant Science* **9,** 105–107.

Babb S, Muehlbauer GJ. 2003. Genetic and morphological characterization of the barley *uniculm2* (*cul2*) mutant. *Theoretical and Applied Genetics* **106,** 846–857.

Boller T, Felix G. 2009. A renaissance of elicitors: perception of microbe-associated molecular patterns and danger signals by pattern-recognition receptors. *Annual Review of Plant Biology* **60,** 379–406.

Buchanan-Wollaston V. 1997. The molecular biology of leaf senescence. *Journal of Experimental Botany* **48,** 181–199.

Close TJ, Wanamaker SI, Caldo RA, Turner SM, Ashlock DA, Dickerson JA, Wing RA, Muehlbauer GJ, Kleinhofs A, Wise RP. 2004. A new resource for cereal genomics: 22K barley GeneChip comes of age. *Plant Physiology* **134,** 960–968.

Close TJ, Wanamaker S, Roose ML, Lyon M. 2007. HarvEST. An EST database and viewing software. *Methods in Molecular Biology* **406,** 161–177.

Corbesier L, Vincent C, Jang S, *et al*. 2007. FT protein movement contributes to long-distance signaling in floral induction of *Arabidopsis*. *Science* **316,** 1030–1033.

Distelfeld A, Korol A, Dubcovsky J, Uauy C, Blake T, Fahima T. 2008. Colinearity between the barley grain protein content (GPC) QTL on chromosome arm 6HS and the wheat *Gpc-B1* region. *Molecular Breeding* **22,** 25–38.

Distelfeld A, Li C, Dubcovsky J. 2009. Regulation of flowering in temperate cereals. *Current Opinion in Plant Biology* **12,** 178–184.

Fu ZQ, Guo M, Jeong B, Tian F, Elthon TE, Cerny RL, Staiger D, Alfano JR. 2007. A type III effector ADP-ribosylates RNA-binding proteins and quells plant immunity. *Nature* **447,** 284–288.

García del Moral LF, Miralles DJ, Slafer GA. 2002. Initiation and appearance of vegetative and reproductive structures throughout barley development. In: Slafer G, Molina-Cano JL, Savin R, Araus JL, Romagosa I, eds. *Barley science: recent advances from molecular biology to agronomy of yield and quality*. Binghamton, NY: Food Products Press, 243–268.

Gregersen PL, Holm PB, Krupinska K. 2008. Leaf senescence and nutrient remobilisation in barley and wheat. *Plant Biology* **10,** Suppl. 1, 37–49.

Heidlebaugh NM, Trethewey BR, Jukanti AK, Parrott DL, Martin JM, Fischer AM. 2008. Effects of a barley (*Hordeum vulgare*) chromosome 6 grain protein content locus on whole-plant nitrogen reallocation under two different fertilisation regimes. *Functional Plant Biology* **35,** 619–632.

Hemming MN, Peacock WJ, Dennis ES, Trevaskis B. 2008. Low-temperature and daylength cues are integrated to regulate *FLOWERING LOCUS T* in barley. *Plant Physiology* **147,** 355–366.

Hensel LL, Grbić V, Baumgarten DA, Bleecker AB. 1993. Developmental and age related processes that influence the longevity and senescence of photosynthetic tissues in Arabidopsis. *The Plant Cell* **5,** 553–564.

Jukanti AK, Fischer AM. 2008. A high-grain protein content locus on barley (*Hordeum vulgare*) chromosome 6 is associated with increased flag leaf proteolysis and nitrogen remobilization. *Physiologia Plantarum* **132,** 426–439.

Jukanti AK, Heidlebaugh NM, Parrott DL, Fischer IA, McInnerney K, Fischer AM. 2008. Comparative transcriptome profiling of near-isogenic barley (*Hordeum vulgare*) lines differing in the allelic state of a major grain protein content locus identifies genes with possible roles in leaf senescence and nitrogen reallocation. *New Phytologist* **177,** 333–349.

Karsai I, Szücs P, Köszegi B, Hayes PM, Casas A, Bedö Z, Veisz O. 2008. Effects of photo and thermo cycles on flowering time in barley: a genetical phenomics approach. *Journal of Experimental Botany* **59,** 2707–2715.

Kim JH, Durrett TP, Last RL, Jander G. 2004. Characterization of the *Arabidopsis* TU8 glucosinolate mutation, an allele of *TERMINAL FLOWER2*. *Plant Molecular Biology* **54,** 671–682.

Lim PO, Kim HJ, Nam HG. 2007. Leaf senescence. *Annual Review of Plant Biology* **58,** 115–136.

Masclaux-Daubresse C, Reisdorf-Cren M, Orsel M. 2008. Leaf nitrogen remobilisation for plant development and grain filling. *Plant Biology* **10,** Suppl. 123–36.

Mickelson S, See D, Meyer FD, Garner JP, Foster CR, Blake TK, Fischer AM. 2003. Mapping of QTL associated with nitrogen storage and remobilization in barley (*Hordeum vulgare* L.) leaves. *Journal of Experimental Botany* **54,** 801–812.

Noh Y-S, Amasino RM. 1999. Identification of a promoter region responsible for the senescence-specific expression of *SAG12*. *Plant Molecular Biology* **41,** 181–194.

Parrott DL, McInnerney K, Feller U, Fischer AM. 2007. Steam-girdling of barley (*Hordeum vulgare*) leaves leads to carbohydrate accumulation and accelerated leaf senescence, facilitating transcriptomic analysis of senescence-associated genes. *New Phytologist* **176,** 56–69.

Schöning JC, Streitner C, Page DR, Hennig S, Uchida K, Wolf E, Furuya M, Staiger D. 2007. Auto-regulation of the circadian slave oscillator component *At*GRP7 and regulation of its targets is impaired by a single RNA recognition motif point mutation. *The Plant Journal* **52,** 1119–1130.

See D, Kanazin V, Kephart K, Blake T. 2002. Mapping genes controlling variation in barley grain protein concentration. *Crop Science* **42,** 680–685.

Strain HH, Cope BT, Svec WA. 1971. Analytical procedures for the isolation, identification, estimation and investigation of the chlorophylls. *Methods in Enzymology* **23,** 452–476.

Streitner C, Danisman S, Wehrle F, Schöning JC, Alfano JR, Staiger D. 2008. The small glycine-rich RNA binding protein AtGRP7 promotes floral transition in *Arabidopsis thaliana*. *The Plant Journal* **56,** 239–250.

Suárez-López P, Wheatley K, Robson F, Onouchi H, Valverde F, Coupland G. 2001. *CONSTANS* mediates between the circadian clock and the control of flowering in *Arabidopsis*. *Nature* **410,** 1116–1120.

Torii KU. 2008. Transmembrane receptors in plants: receptor kinases and their ligands. *Annual Plant Reviews* **33,** 1–29.

Trevaskis B, Hemming MN, Dennis ES, Peacock WJ. 2007. The molecular basis of vernalization-induced flowering in cereals. *Trends in Plant Science* **12,** 352–357.

Uauy C, Distelfeld A, Fahima T, Blechl A, Dubcovsky J. 2006. A NAC gene regulating senescence improves grain protein, zinc, and iron content in wheat. *Science* **314,** 1298–1301.

Wingler A, Purdy SJ, Edwards S-A, Chardon F, Masclaux-Daubresse C. 2010. QTL analysis for sugar-regulated leaf senescence supports flowering-dependent and -independent senescence pathways. *New Phytologist* **185,** 420–433.

Wu K, Zhang I, Zhou C, Yu C-W, Chaikam V. 2008. HDA6 is required for jasmonate response, senescence and flowering in Arabidopsis. *Journal of Experimental Botany* **59,** 225–234.